The Electronic Structure and Homolytic Dissociation of Dibenzoyl Peroxide

Osamu KIKUCHI, Akihisa HIYAMA, Hiroshi YOSHIDA, and Keizo SUZUKI

Institute of Chemistry, The University of Tsukuba, Sakura-mura, Ibaraki 300-31

(Received May 12, 1977)

The conformations and electronic structures of dibenzoyl peroxide (BPO) and the benzoyloxyl radical (PhCOO) were elucidated by means of closed-shell and restricted open-shell SCF MINDO/3 calculations. The dihedral angle of BPO between the two PhCOO planes was predicted to be 115°, and the barrier to the *trans* form of BPO was estimated to be very small. The ground state of the PhCOO radical was predicted to be of the Σ-type. The non-planar conformation of PhCOO was more stable (2 kcal/mol) than the planar one. The variation in the radical-pair property of the lowest state of acetyl peroxide during the homolytic dissociation process was estimated by the analysis of the two-configuration wavefunctions. The substituent effect on the rate of the homolytic dissociation of BPO was discussed in terms of the electronic structures of substituted BPO.

Dibenzoyl peroxide (BPO) undergoes a variety of reactions because of its weak peroxy O–O bond. A typical process is the simple homolytic cleavage of the O–O bond to form benzoyloxyl radicals:

$$C_6H_5\text{-}\overset{\overset{O}{\|}}{C}\text{-}O\text{-}O\text{-}\overset{\overset{O}{\|}}{C}\text{-}C_6H_5 \longrightarrow 2C_6H_5\text{-}\overset{\overset{O}{\|}}{C}\text{-}O\cdot \qquad (1)$$

Numerous investigations[1] have been experimentally performed on the mechanism of (1) and of the successive reactions. The substituent effect[2] on Reaction (1) has been observed; the rate constant correlates with the Hammet σ constant with $\rho=-0.38$. This substituent effect was explained in terms of the electrostatic repulsion between the two peroxy oxygen atoms[2] or that between the two carbonyl oxygen atoms.[3] These explanations are qualitative ones, and no MO-theoretical studies have been reported on the electronic structures of BPO and the benzoyloxyl radical[4] in connection with the dissociation process of BPO. The purposes of this paper are (i) to examine the electronic structures of BPO, substituted BPO, and the benzoyloxyl radical; (ii) to explain the substituent effect on the rate of the O–O cleavage in terms of the electronic structure of BPO, and (iii) to consider the variation in the electronic structure of BPO during its homolytic dissociation process. The results obtained here will be useful for the understanding of a variety of reactions involving BPO and the benzoyloxyl radical.

Method

The MINDO/3 method[5] was employed to determine the most favorable conformation of BPO. Since a large number of geometrical parameters are involved in BPO, the geometry of diacetyl peroxide (APO) was first optimized; the parameters obtained for the COO groups in APO were then employed in the calculations of BPO. The bond lengths and bond angles of the phenyl groups (CC=1.397 Å, CH=1.087 Å, CCC=CCH=120°)[6] were not optimized. Only two parameters, the peroxy O–O bond length and the dihedral angle between the two PhCOO planes, were optimized. The total energy of BPO was partitioned into atomic energies and atom-atom energies in order to elucidate the electronic factors affecting the conformation of BPO. According to Fischer and Kollmar,[7] the total energy of a molecule can be partitioned into one-center and two-center terms:

$$E_{\text{total}} = \sum_{A} E_A + \sum_{A>B} E_{A,B}, \qquad (2)$$

where the two-center energy between the A and B atoms can be written in the form:[7]

$$E_{A,B} = E^{R}_{A,B} + E^{K}_{A,B} + (E^{J}_{A,B} + E^{V}_{A,B} + E^{N}_{A,B}). \qquad (3)$$

$E^{R}_{A,B}$ is the contribution of the resonance integrals to $E_{A,B}$, $E^{K}_{A,B}$ is the corresponding term of the electronic exchange interaction, and the third term in parentheses is the electrostatic interaction energy between the A and B atoms.

The conformation and electronic structure of the benzoyloxyl radical (PhCOO) were discussed on the basis of the interactions between the MO's of the phenyl radical and those of the bent COO fragment. These discussions were supported by the restricted open-shell SCF calculations with the MINDO/3 approximation. The open-shell SCF method employed was the approximate one proposed by Longuet-Higgins and Pople.[8] The general SCF theory,[9] which gives correct variational solutions for the open-shell problems, was also used to confirm the results obtained by the approximate open-shell SCF calculations.

The small configuration interation (CI) calculations, in which only two configurations related to the σ and σ^* MO's of the peroxy O–O bond were taken into account, were carried out to obtain the qualitative potential curves during the dissociation process (1). As may be seen from Fig. 1, the energy difference between the σ and σ^* orbitals of the peroxy O–O bond becomes small when the O–O distance, R_{OO}, increases.

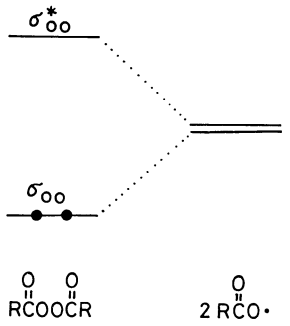

Fig. 1. The correlation diagram for the peroxy O–O σ orbitals along the dissociation process.

Therefore, reliable potential curves of acyl peroxide along the O–O bond cleavage cannot be obtained by the single-configuration wavefunction:[10]

$$\Psi_g = |\cdots\sigma^2\sigma^{*0}|, \quad (4)$$

$$\sigma = \frac{1}{\sqrt{2}}(\chi_a + \chi_b), \quad (5)$$

$$\sigma^* = \frac{1}{\sqrt{2}}(\chi_a - \chi_b), \quad (6)$$

where χ_a and χ_b are the AO's of the two peroxy oxygen atoms, whose directions are parallel to the O–O bond. Near the equilibrium O–O distance, the ground state of acyl peroxide can well be described by Ψ_g, and the mixing of Ψ_g with the excited configuration:

$$\Psi'' = |\cdots\sigma^0\sigma^{*2}|, \quad (7)$$

is very small. When R_{OO} increases, the mixing between Ψ_g and Ψ'' becomes very large and a linear combination of them must be used for the wavefunction of the lowest state. The potential curves were thus calculated by the CI calculations in which Ψ_g and Ψ'' were included. The two-configuration wavefunctions were then analyzed, and the radical-pair property of the RCOO–OOCR system was estimated during the dissociation process of (1).

Results and Discussion

Conformation of BPO. The most stable conformation of BPO predicted by MINDO/3 is shown in Fig. 2. The predicted O–O distance, 1.41 Å, is smaller than the observed value[11] by 0.05 Å, and the dihedral angle, 115°, is slightly larger than the observed value (≃90°)[11] of BPO. It is interesting that these values are identical with those predicted for APO, despite the large difference in the substituents of BPO and APO. Figure 3 shows the energy variations of BPO and APO with respect to the rotation angle about the peroxy O–O bond. The barrier to a *cis* form was very large(≈40 kcal/mol), while that to a *trans* form was very small (1 kcal/mol).

Three factors may be important in analyzing the favorable conformation of BPO: (i) Electron delocalization over both the COO groups through the peroxy O–O bond; (ii) electro-static repulsion between the two carbonyl oxygen atoms, which makes the dihedral angle large, and (iii) the interaction between the lone-pair electrons of the peroxy O–O atoms, which is sensitive to the dihedral angle. These factors were examined on the basis of the partitioned energies. The large dependence upon the dihedral angle, θ, was recognized in the two-center energies between two peroxy oxygen atoms and in those between two carbonyl groups. In Fig. 4, the two-center energy between the two peroxy oxygen atoms, $E_{1,5}$, and that between two carbonyl oxygens, $E_{3,7}$, are plotted. The electrostatic repulsion between two peroxy oxygens, $E^J_{1,5}+E^V_{1,5}+E^N_{1,5}$, was almost constant at any value of θ, because the atomic electron densities of the peroxy oxygen atoms were almost constant to the rotation angle. The lowering of $E_{1,5}$ in the region of θ=60—90° comes from the stabilization of the O–O bond due to the resonance energy:

$$E^R_{1,5} = 2\sum_{r,s} P_{rs}H^{core}_{rs}, \quad (8)$$

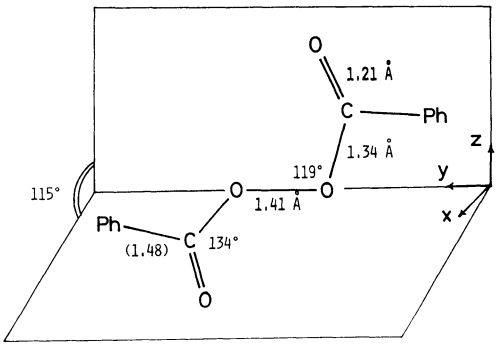

Fig. 2. The predicted geometry of BPO.

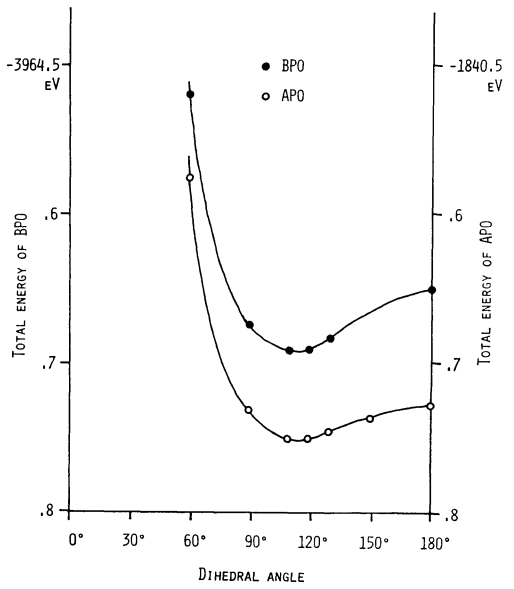

Fig. 3. Dependence of total energies of BPO and APO upon the dihedral angle between two RCOO planes.

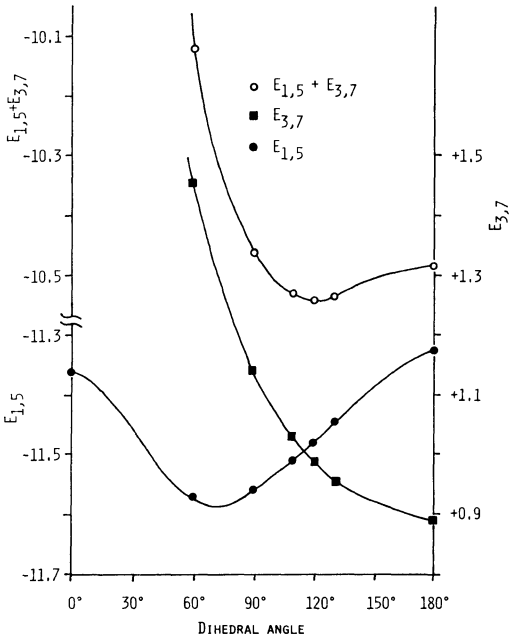

Fig. 4. Dependence of two-center energies of BPO upon the dihedral angle between two PhCOO planes.

Table 1. Electron densities on the COO groups and bond orders between the peroxy oxygen atoms in substituted BPO[a)]

R_1	R_2	Atomic electron density[b)]						Bond order[c)]	
		O1	O5	C2	C6	O3	O7	$P_{1y,5y}$	$P_{1x,5x}+P_{1z,5z}$
OCH_3	OCH_3	6.270	6.270	3.207	3.207	6.570	6.570	0.8933	0.1695
OCH_3	H	6.269	6.267	3.206	3.215	6.570	6.565	0.8932	0.1701
CH_3	CH_3	6.267	6.267	3.215	3.215	6.564	6.564	0.8932	0.1708
CH_3	H	6.267	6.266	3.215	3.215	6.564	6.564	0.8932	0.1708
H	H	6.268	6.268	3.215	3.215	6.562	6.562	0.8932	0.1705
CN	H	6.266	6.266	3.217	3.217	6.559	6.561	0.8932	0.1710
CN	CN	6.266	6.266	3.217	3.217	6.558	6.558	0.8933	0.1711
NO_2	H	6.267	6.264	3.221	3.216	6.548	6.558	0.8931	0.1716
NO_2	NO_2	6.263	6.263	3.219	3.219	6.547	6.547	0.8932	0.1723
OCH_3	NO_2	6.267	6.267	3.208	3.221	6.565	6.549	0.8930	0.1710

a) The geometry of unsubstituted BPO predicted in this paper was employed in the calculations.

b) 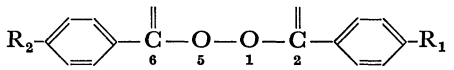

c) The axes, x, y, and z, are shown in Fig. 1. The positive values correspond to the bonding character.

where P_{rs} and H_{rs}^{core} have the usual meanings. The resonance energy between peroxy oxygens decreases (becomes more stable) as a result of the mixing of the lone-pair electrons with the π-electrons of the adjacent carbonyl group.

The electrostatic repulsion energy between two carbonyl oxygens decreases rapidly with increase in θ, because the distance between two carbonyl oxygens increases with θ. This electrostatic energy is dominant in $E_{3,7}$. The angular dependence of $E_{1,5}+E_{3,7}$ shown in Fig. 4 resembles that of the total energy of BPO shown in Fig. 3 The dihedral angle of BPO can thus be interpreted in terms of two factors, the electrostatic repulsion energy between two carbonyl oxygens and the resonance energy between two peroxy oxygens.

Electron Distribution in BPO. Since the rate of the dissociation of BPO depends on the substituents introduced in the phenyl group,[2)] it is worthwhile examining the electronic structures of substituted BPO. Nine substituted BPO were calculated using the conformation of unsubstituted BPO shown in Fig. 2. The electron densities on the carbonyl and peroxy groups and the bond orders between the peroxy oxygen atoms are listed in Table 1. The electron densities appear to reflect gently the characters of the substituents; the electron-withdrawing group, for example, reduces the electron densities on both the peroxy and carbonyl oxygen atoms. The bond order between AO's whose directions are perpendicular to the O–O bond also reflects the characters of the substituents. The effect of CH_3 groups on the electron distribution is very small, perhaps because the $(COO)_2$ group itself has an electron-donating character.

Electronic Structure of the Benzoyloxyl Radical. The energy levels and qualitative pictures of the MO's of the C_∞ CO_2 molecule and those of the bent C_{2v} COO fragment are shown in Fig. 5. A reduction of the symmetry property of CO_2 from C_∞ to C_{2v} causes (i) a rise in the orbital energies of π° and $\bar{\pi}^\circ$ orbitals because of the anti-bonding interaction between the terminal p orbitals, and (ii) a lowering of the 5σ orbital due to the strong mixing of this orbital with the $\bar{\pi}^*$ orbital. Since the instabilization of the $\bar{\pi}^\circ$ orbital is larger than that of the π° orbital, an inversion of the MO levels of $4a_1$ and $3b_2$ is expected for the small OCO angle ($<120°$).

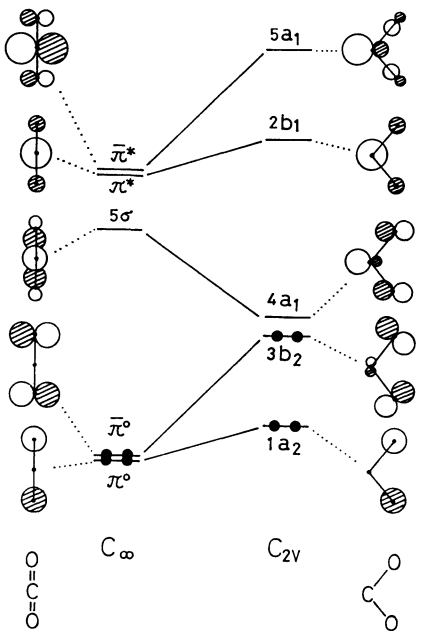

Fig. 5. Energy levels and qualitative pictures of some higher-occupied and lower-unoccupied MO's of the C_∞ CO_2 molecule and the bent CO_2 fragment.

The stability of the PhCOO radical can be elucidated by the interaction between the bent COO fragment and the phenyl radical. The half-occupied MO of the phenyl radical interacts with the unoccupied $4a_1$ MO of COO to form the Ph–COO bond. Since only one electron occupies the newly formed PhCOO bond, the $^2A_1$ state of PhCOO can be expected to break its Ph–COO bond easily to produce the phenyl radical

and CO_2. One-electron migration from the doubly-occupied $3b_2$ orbital to the half-occupied $4a_1$ orbital of the PhCOO radical makes the Ph–COO bond strong. Thus, the stable $^2B_2$ state of the PhCOO radical is expected for the small OCO angle. Since a larger energy is required for the electron migration from la_2 (π) to $4a_1$, the $^2A_2$ state (π-radical) of PhCOO can be expected to be more unstable than the $^2B_2$ state.

The above qualitative discussions were supported by open-shell SCF calculations. Calculations were performed by restricting the COO geometry of PhCOO to C_{2v}. When the OCO angle is 100—120°, the lowest state of PhCOO was predicted to be the $^2B_2$ state (the σ-radical whose unpaired electron occupies the $3b_2$ orbital shown in Fig. 5). When the OCO angle is larger than 130°, the lowest state was $^2A_1$ (σ-radical) and the Ph–COO bond length becomes long. This indicates that the lowest state for OCO>130° is the intermediate stage in the decarboxylation process of PhCOO. The π-state was higher than the σ-state for the entire range of OCO angles. Recently, the σ-ground state of the acyloxyl radical was predicted by semi-empirical NDDO calculations of HCOO and CH_3-COO[12] and by *ab initio* STO-3G calculations of H-COO.[13] However, the σ-ground state predicted in these studies is a distorted one (C_s symmetry), in which the two C–O bond lengths differ from one another. In the present MINDO/3 calculations, the energy lowering caused by the distortion of the OCO geometry was not observed even if the general SCF theory was employed.

The energy dependence of the lowest $^2B_2$ state of PhCOO upon the dihedral angle between the phenyl and COO planes was calculated. The non-planar conformations were more stable than the planar one. When the two planes were perpendicular to each other, the PhCOO radical was the most stable. However, the barrier to the rotation about the Ph–COO bond was very small (2 kcal/mol). The spin delocalization from the COO group into the phenyl group was very small (less than 0.5%) for both the planar and non-planar PhCOO radicals.

Potential Curves and Radical-pair Property during the Homolytic Dissociation. Variations in the electronic properties of APO during the homolytic dissociation process were examined by two-configuration CI calculations in which Ψ_g and Ψ'' were included. The potential curves obtained are shown in Fig. 6, while the wavefunctions of the lowest state are listed in Table 2. It may be seen from Table 2 that the lowest wavefunction at $R_{OO}=\infty$ is

$$\Phi_\infty = \frac{1}{\sqrt{2}}\{\Psi_g - \Psi''\}. \tag{9}$$

This state can be analyzed by expressing the wavefunction in terms of the orbitals of two separate fragments:[14]

$$\Phi_\infty = |\cdots\chi_a^1| \times |\cdots\chi_b^1|, \tag{10}$$

using Eqs. 4—7. It is clear that this wavefunction corresponds to the two-radical, or the radical-pair, state, and that the ground state of acyl peroxide correlates with a pair of acyloxyl radicals at $R_{OO}=\infty$.

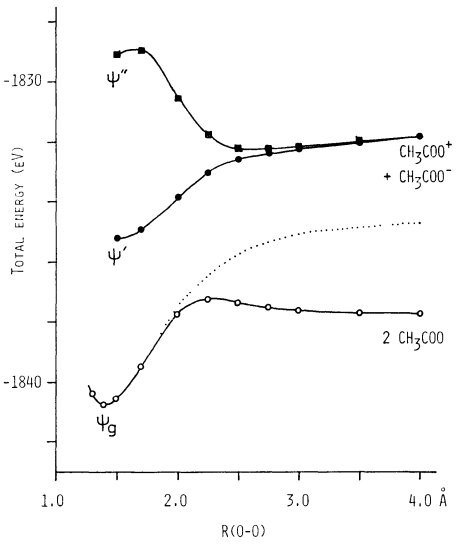

Fig. 6. Potential curves for APO obtained by 2-configuration CI calculations. The dotted line indicates the energy of the single-configuration wavefunction. The Ψ' line corresponds to the electron configuration of $(\cdots\sigma^1\sigma^{*1})$.

TABLE 2. VARIATION IN THE LOWEST WAVEFUNCTION OF APO DURING THE DISSOCIATION OF THE PEROXY O-O BOND

R_{OO} (Å)	Total energy (eV)	Coeffeicients of Ψ_g	Coeffeicients of Ψ''	Radical-pair property (%)
1.30	−1840.378	0.9997	−0.0239	2.5
1.41	−1840.739	0.9996	−0.0285	2.9
1.50	−1840.551	0.9994	−0.0357	3.7
1.70	−1839.469	0.9978	−0.0671	7.2
2.00	−1837.761	0.9857	−0.1685	19.5
2.25	−1837.253	0.9239	−0.3827	50.0
2.50	−1837.342	0.8339	−0.5520	76.5
2.75	−1837.513	0.7723	−0.6353	89.4
3.00	−1837.625	0.7403	−0.6723	95.0
4.00	−1837.750	0.7105	−0.7037	99.5

Similar treatment is possible for the degenerate states at $R_{OO}=\infty$. They correspond to the ionic states: $RCOO^+$ plus $RCOO^-$ and $RCOO^-$ plus $RCOO^+$.

Since the wavefunction of APO at $R_{OO}=\infty$, $(\Psi_g-\Psi'')/\sqrt{2}$, represents the pure radical-pair, the contribution of this term to the lowest state may be a measure of the radical-pair property of the RCOO–OOCR system. In this sense, the radical-pair property involved in the lowest state of APO was analyzed during the dissociation process. The wavefunction at an arbitrary R_{OO} is expressed by:

$$\Phi \equiv c\Psi_g - d\Psi'' = (c-d)\Psi_g + \sqrt{2}d\left\{\frac{1}{\sqrt{2}}(\Psi_g-\Psi'')\right\}, \tag{11}$$

with $c^2+d^2=1$. The radical-pair property of Φ is thus expressed by:

$$(\sqrt{2}d)^2\left\langle \frac{1}{\sqrt{2}}(\Psi_g-\Psi'') \middle| \frac{1}{\sqrt{2}}(\Psi_g-\Psi'') \right\rangle + (c-d)\sqrt{2}d\left\langle \Psi_g \middle| \frac{1}{\sqrt{2}}(\Psi_g-\Psi'') \right\rangle = d^2 + cd, \quad (12)$$

and the covalent-bond property is similarily expressed by c^2-cd. The calculated radical-pair properties of APO during the homolytic dissociation process are listed in Table 2. When $R_{OO}>2.25$ Å, the RCOO–OOCR system can be considered to be a weakly interacting radical pair, while for $R_{OO}<2.25$ Å the covalent-bond property of RCOO–OOCR increases rapidly.

The dissociation energy and the activation energy calculated for the O–O bond cleavage of APO is considerably larger than the observed value ($\simeq$30 kcal/mol).[1,2] In Fig. 6, a large activation energy is predicted for the recombination process of the active acetyloxyl radical. These results may come from the method of calculation employed here where (i) only small configurations were taken into account; (ii) the geometrical parameters involved were not optimized during the dissociation process, and (iii) the inaccuracy inherently involved in the MINDO/3 approximation was not estimated. Thus, any quantitative discussion about the reaction energies may be risky.

Substituent Effect on the Dissociation of BPO. Swain *et al.*[2a] studied the dissociation process of many substituted BPO and found that the electron-withdrawing substituents reduced the rate of the dissociation, while the electron-donating substituents increased the rate. This effect was explained[2a] in terms of the electrostatic repulsion between the two peroxy oxygen atoms, which is reduced by the electron-withdrawing group and which is increased by the electron-donating group. The calculated results (Table 1) reflect the substituent effect pointed out by Swain *et al.* However, the effect is very small. The importance of the electrostatic repulsion between the carbonyl oxygen atoms was pointed out by Imoto.[3] The calculated results show that the electron-donating group increases the repulsion energy between carbonyl oxygens. However, as may be seen from Fig. 3, the barrier to the *trans* form of BPO is expected to be very small, and the increased repulsion between carbonyl oxygens is compensated for by increasing of the dihedral angle, θ.

The bond order between peroxy oxygen atoms, $P_{1y,5y}$, shown in Table 1 is almost constant and fails to explain the substituent effect on the dissociation rate.

Another explanation is more reasonable. When the electron-donating group is introduced to the phenyl group, the electron densities on the carbonyl oxygen atoms increase (Table 1) and the electrostatic repulsion between the oxygen atoms increases. This makes the dihedral angle, θ, large without any appreciable loss of energy, since the barrier to the *trans* form is very small (Fig. 3). The resonance energy between the O–O atoms increases (becomes more unstable) with the increase in the dihedral angle (Fig. 4). As a result, the introduction of the electron-donating group into the phenyl group makes the peroxy bond weak and makes the dissociation of the O–O bond easy.

The radical-pair property defined here may be a measure of the weakness of the O–O bond of BPO. A substituted BPO, in which a large radical-pair property is inherently involved, can be expected to have a low activation energy. The calculated radical-pair properties of *p,p'*-dinitro-BPO (1.5%), unsubstituted BPO (2.1%), *p,p'*-dimethoxy-BPO (2.2%), and APO (2.9%) agreed with the trend of the experimental rates of the dissociation.

One of the authors, O. K., wishes to express his thanks to Professor Katsumi Tokumaru and to Dr. Ken Fujimori for their useful suggestions.

References

1) T. Koenig, "Free Radicals I," ed by J. K. Kochi, John Wiley & Sons, New York (1973), p. 113; Y. Ogata, "Chemistry of Organic Peroxides," Nankodo, Tokyo (1971), p. 170.

2) (a) C. G. Swain, W. H. Stockmayer, and J. T. Clarke, *J. Am. Chem. Soc.*, **72**, 5426 (1950) ; (b) A. T. Blomquist and A. J. Buselli, *J. Am. Chem. Soc.*, **73**, 3883 (1951).

3) M. Imoto, "Theory of Organic Reactions," Kyoritsu Shuppan, Tokyo (1961), p. 430.

4) INDO calculations of BPO were reported by N. J. Karch, E. T. Koh, B. L. Whitsel, and J. M. McBride, *J. Am. Chem. Soc.*, **97**, 6729(1975).

5) R. C. Bingham, M. J. S. Dewar, and D. H. Lo, *J. Am. Chem. Soc.*, **97**, 1285, 1294, 1302, 1307 (1975).

6) E. Sutton, "Tables of Interatomic Distances," Special Publications No. 11, The Chemical Society, London (1958).

7) H. Fischer and H. Kollmar, *Theor. Chim. Acta*, **16**, 163(1970).

8) H. C. Longuet-Higgins and J. A. Pople, *Proc. Phys. Soc.*, **68**, 591(1955).

9) K. Hirao and H. Nakatsuji, *J. Chem. Phys.*, **59**, 1457 (1973).

10) O. Kikuchi and K. Aoki, *Bull. Chem. Soc. Jpn.*, **47**, 2915 (1974).

11) M. Sax and R.K. McMullan, *Acta Crystallogr.*, **22**, 281 (1967); W. Lobunez, J. R. Rittenhouse, and J. G. Miller, *J. Am. Chem. Soc.*, **80**, 3505 (1958).

12) O. Kikuchi, K. Utsumi, and K. Suzuki, *Bull. Chem. Soc. Jpn.*, **50**, 1399(1977).

13) O. Kikuchi, *Tetrahedron Lett.*, **1977**, 2421.

14) O. Kikuchi, *Chem. Lett.*, **1972**, 1121.